Dynamic-decision-based Real-time Dispatch for Reducing Constraint Violations

Lingshu Zhong, Junbo Zhang, C. Y. Chung, Yuzhong Gong, and Lin Guan

***Abstract*—This paper proposes a dynamic-decision-based real-time dispatch method to coordinate the economic objective with multiple types of security dispatch objectives while reducing constraint violations in the process of adjusting the system operation point to the optimum. In each decision moment, the following tasks are executed in turn: ① locally linearizing the system model at the current operation point with the online model identification by using measurements; ② narrowing down the gaps between unsatisfied security requirements and their security thresholds in order of priority; ③ minimizing the generation cost; ④ minimizing the security indicators within their security thresholds. Compared with the existing real-time dispatch strategies, the proposed method can adjust the deviations caused by unpredictable power flow fluctuations, avoid dispatch bias caused by model parameter errors, and reduce the constraint violations in the dispatch decision process. The effectiveness of the proposed method is verified with the IEEE 39-bus system.**

***Index Terms*—Dynamic decision, real-time dispatch, security-constrained dispatch, *N*–1 security, small-signal stability, data-driven optimization.**

I. Introduction

THE conventional power system dispatch is determined by off-line system models and predicted operation conditions every 5 min or longer to maintain the system under reliable and secure conditions with the minimum economic and environmental costs [1]. With the increasing uncertainties introduced into modern power grids, off-line model parameters and predicted operation conditions might deviate far from the actual values [2], [3], so that the generations scheduled in advance may deviate from the optimum or even fall into the insecure region [4]. Two kinds of technologies are proposed to handle these deviations at different time scales. Stochastic and robust dispatch strategies [5], [6] provide the moderate generation scheduling for possible operation conditions in advance that can mitigate the security risks caused by these deviations, while the real-time dispatch is used to continuously drive the operation point of the system to a new optimal one with actual operation conditions and online identified model parameters [7], [8].

Since power fluctuations are almost unpredictable in the real-time scale, existing real-time dispatch strategies are often single-period. The optimal operation point is calculated at each decision moment, and the generator outputs will be regulated towards it as much as possible until the next decision moment. In this case, the system will gradually approach the optimal operation point as shown in Fig. 1.

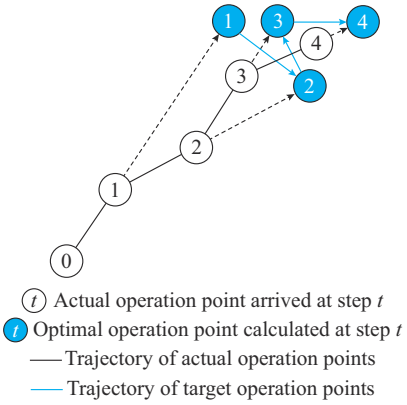

Fig. 1. Moving track of operation point during real-time dispatch.

To simultaneously consider the comprehensive economic and security requirements such as costs, static security [9], and small-signal stability [10], the security operation region will be narrowed down, which would cause the challenges of constraint violations to the existing real-time dispatch strategies.

An example of constraint violations is given in Fig. 2. The security boundary looks peculiar due to the comprehensive security requirements. If the system operation condition remains static in a few periods, the current system operation point will move towards the optimal operation point through path 1 with existing real-time dispatch methods. In this case, the system will return to the security region at the fifth decision moment just before it reaches the optimal operation point, which may be an acceptable result if a longer period of constraint violations is tolerated. However, if the duration of the constraint violations is wanted to be reduced, the path

Manuscript received: August 4, 2020; revised: November 1, 2020; accepted: January 11, 2021. Date of CrossCheck: January 11, 2021. Date of online publication: July 27, 2021.

This work was supported by the National Natural Science Foundation of China (No. 51761145106), the Guangdong Provincial Natural Science Foundation of China (No. 2018B030306041), the Fundamental Research Funds for the Central Universities (No. 2019SJ01), and the China Scholarship Council (No. 201806155019).

L. Zhong, J. Zhang (corresponding author), and L. Guan are with the School of Electrical Power, South China University of Technology, Guangzhou 510640, China (e-mail: z.lingshu@mail.scut.edu.cn; epjbzhang@scut.edu.cn; lguan@scut.edu.cn).

C. Y. Chung and Y. Gong are with the Department of Electrical and Computer Engineering, University of Saskatchewan, Saskatoon S7N5A9, Canada (e-mail: c.y.chung@usask.ca; y.z.gong@usask.ca).

DOI: 10.35833/MPCE.2020.000580

2 is much preferred, which requires one more period to reach the optimal operation point but can recover the system security within only one period.

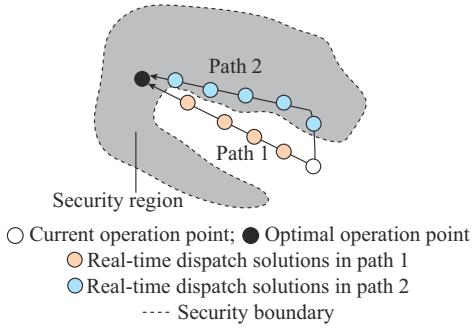

Fig. 2. An example of constraint violation problem.

In practice, the system operation conditions may hardly remain constant so that the benefit of moving the system operation point directly towards a temporary and distant optimum at every decision moment will be even less. If the operation condition fluctuates wildly, following up with these fluctuations and continuously tracking the optimal operation points will be impossible. As a result, the choice of actually reducing the constraint violations while improving other dispatch objectives will be more meaningful.

Moreover, with the increasing number of economic and security requirements to be considered, the possibility of simultaneous violation of multiple constraints is increasing. In this case, the coordination and the tradeoff should be made among different dispatch objectives at each decision moment to ensure the most urgent security problem is solved with the highest priority. In this case, the objective function of the dispatch problem needs to be regulated dynamically, leading to a dynamic-decision-based real-time dispatch problem.

This paper proposes a novel dynamic-decision-based real-time dispatch method that minimizes the number of constraint violations at each decision moment while tracking the optimal operation points. Besides, more merits include: ① handling the priority of different dispatch objectives at different operation points; ② approximating the system model in a measurement-based way to reduce the computational complexity; ③ simultaneously considering the generation cost, N–1 line loading, and damping ratios of the system.

Contributions of this paper include two aspects.

1) A multi-objective real-time dispatch model is proposed to consider three categories of typical dispatch objectives and the constraint violations while moving the operation point towards the optimum.

2) A decision-based solution method is proposed to solve the proposed dispatch model in real time, while the priority of different security objectives can be set in advance.

The remainder of this paper is organized as follows. Section II presents a brief review of existing dispatch strategies. Section III describes the proposed dispatch model to handle multiple dispatch objectives considering constraint violations. Section IV gives the solution method for the proposed model to make the optimal dispatch decision at each decision moment. Section V tests the proposed model and solution with three study cases. Section VI concludes this paper.

II. Brief Review of Existing Dispatch Strategies

Different economic or security indicators should be considered in dispatch strategies to achieve different dispatch objectives. There are many different forms of these indicators, which fall into three categories as follows.

1) Indicators with predetermined model parameters are independent of either system dynamics or operation conditions. Economic and environmental objectives often consider this type of the indicators.

2) Indicators with model parameters are only related to the system topology and the impedance. Static security objectives often consider this type of indicators.

3) Indicators are related to system dynamics. Dynamic security objectives belong to this category.

Since dispatch objectives in the same category often consider similar indicators, three typical dispatch objectives are used to consider the aforementioned three categories of economic or security indicators, respectively: generation cost reduction, static security, and small-signal stability. Figure 3 shows the development of dispatch strategies considering these typical objectives.

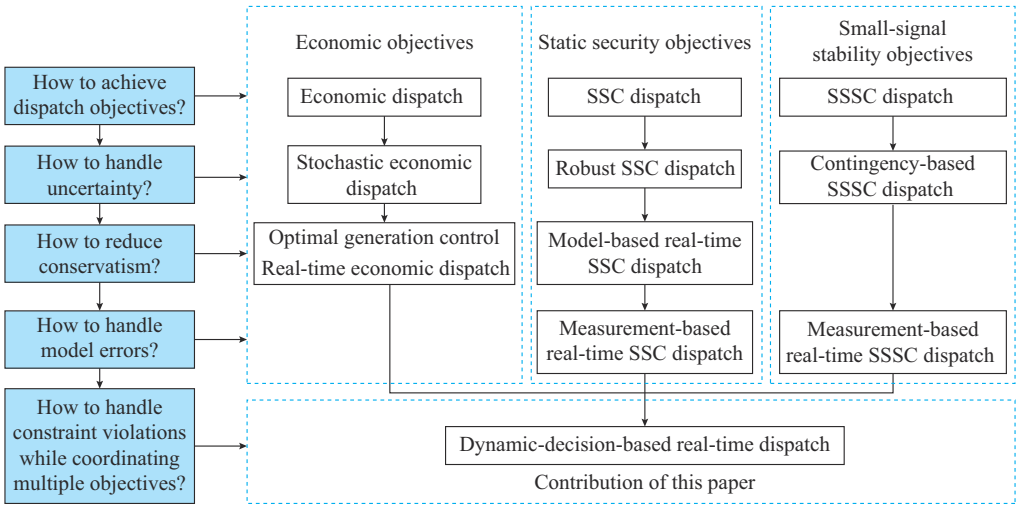

Fig. 3. Development of dispatch strategies.

A. Generation Cost Reduction

The generation cost is often formulated as the objective function of the economic dispatch (ED) strategy, where all the parameters are given in advance [1]. To handle the uncertainties caused by prediction errors and power fluctuations, different technologies are put into practice on different time scales.

On a longer time scale, the stochastic optimization is introduced to minimize the mathematical expectation of the generation cost in advance based on the probability distribution of potential operation conditions, leading to stochastic dispatch strategies [11]. With the high penetration of different types of renewable energy resources, more probability models and cost functions have been developed, such as underestimated and overestimated costs [12], the Markov chain based distributional forecast model [13], and the cumulative distribution function of the wind power [5].

While the generation schedules obtained by stochastic methods minimize the expectation of generation cost for possible scenarios, the real-time dispatch is used to get a further optimization on the actual generation cost for each particular scenario on a shorter time scale [14]-[16]. In this case, the total generation cost can be minimized with the distributed optimal generator control to get the better real-time performance. For instance, a multi-agent-based distributed control method is presented in [17] to realize the optimal automatic generation control (AGC). In [18], a combined AGC and ED control methodology is investigated with control areas containing multiple hybrid energy resources. A distributed economic predictive control model is proposed in [19] for economic load dispatch and load frequency control of interconnected power systems.

B. Static Security

N–1 line loadings and other static security objectives are often formulated as constraints of the dispatch problem and handled by static security-constrained (SSC) dispatch strategies [20]. To eliminate the security risks brought by uncertain power fluctuations, the robust optimization is introduced to ensure system static security requirements even under the worst operation conditions. In [6], a hierarchical robust security-constrained unit commitment of multi-area power systems is proposed with an uncertainty set specified by the variance of the system net load. A statistical ranking methodology that allows adaptive robust stochastic unit commitment using a modular structure with the needed flexibility is proposed in [21]. A long-term robust co-optimization planning model is presented in [22] for interdependent systems considering both *N*–1 and probabilistic reliability criteria.

The single-stage robust dispatch often suffers from the drawback of over-conservativeness since the scheduled generator outputs will be optimal only for the worst operation condition. To solve this problem, the real-time dispatch is used as a second-stage dispatch to adjust the generation in actual operation conditions. In [23], a data-driven distributionally robust chance-constrained real-time dispatch considering renewable generation forecasting errors is proposed. A look-ahead real-time ED strategy is formulated in [24] by using a new scenario approach. A confidence interval based distributionally robust real-time ED approach is proposed in [25], which considers the risk related to the accommodated wind power. Different from the generation cost, the calculation of *N*–1 line loadings is disturbed by the prediction errors and the errors of static model parameters. To adjust the deviation, a measurement-based real-time dispatch is proposed in [7].

C. Small-signal Stability

The small-signal stability problem is one of the significant threats to the security and reliability of the power system. An unstable mode can cause violent oscillations and lead to large-scale blackouts. To avoid this situation, maintaining a sufficient small-signal stability margin becomes an important dispatch objective, which leads to the birth of small-signal stability constrained (SSSC) dispatch strategies [26]. In an SSSC dispatch strategy, damping ratios representing dynamic security margins in different stressed operation conditions are maintained at a high enough level [26], [27]. Different from the generation cost and *N*–1 line loadings, the calculation of damping ratios or other dynamic security objectives depends on the dynamic system model, which is highly nonconvex and difficult to be obtained. Different sequential approaches are used to handle the model nonconvexity and search for the global optimization [28], [29], while measurement-based real-time dispatch strategies are used to handle the model error and inaccessibility [8], [30]. Since the complete dynamic model of the system is impossible to be identified by the measurement, the sensitivity-based local approximation models near the actual operation points are used instead.

The dispatch strategies mentioned above can handle different typical dispatch objectives, while the tools that can be used in real time considering all three types of objectives under the uncertainties from both the power flow and model parameters are very limited. Stochastic methods like the stochastic optimization and the robust optimization require a system model that can be used in hypothetical operation conditions far from the actual operation point. In this case, only deterministic measurement-based real-time methods can be used.

In existing real-time dispatch strategies, the security objectives are formulated as constraints. As a result, different types of security objectives may lead to constraint violations, as mentioned in the introduction part. Therefore, a new method is proposed in this paper to solve this problem by coordinating the priorities of different security objectives.

III. Dynamic-decision-based Real-time Dispatch

In this section, a dynamic-decision-based real-time dispatch model is proposed, which considers multiple security and economic indicators, as well as their priorities.

A. Considered Dispatch Objectives

The typical security indicators mentioned in Section II, i.e., the generation cost, line loadings in *N*–1 conditions, and the damping ratios, are chosen as dispatch objectives formu-

lated in the dispatch model. Considering a system that consists of N buses indexed by $n \in \mathcal{N} = \{1, 2, \ldots, N\}$, G generators indexed by $g \in \mathcal{G} = \{1, 2, \ldots, G\}$, D loads indexed by $d \in \mathcal{D} = \{1, 2, \ldots, D\}$, L transmission lines indexed by $l \in \mathcal{L} = \{1, 2, \ldots, L\}$, and J dominant oscillation modes indexed by $j \in \mathcal{J} = \{1, 2, \ldots, J\}$, the indicators can be formulated as follows.

1) Generation Cost

For each generator g, the generation cost can be expressed as a quadratic function of its active power output:

$$f(\boldsymbol{x}) = \sum_{g \in \mathcal{G}} (a_g x_g^2 + b_g x_g + c_g) \tag{1}$$

where a_g, b_g, and c_g are the cost coefficients; and $\boldsymbol{x}$ is the decision vector, among which $x_g \in \boldsymbol{x}$ is the active power generation of the generator g.

2) Line Loading Indicators

For each transmission line u, the line loading indicator P_u^{L} denotes the active power transmitted through it and the security threshold $P_{u,\max}^{\mathrm{L}}$ denotes its rated line capacity. The line loading indicators can be formulated as a linear function:

$$\boldsymbol{P}^{\mathrm{L}} = \boldsymbol{\sigma} \boldsymbol{P}^{\mathrm{N}} \tag{2}$$

where $\boldsymbol{P}^{\mathrm{L}}$ is the vector of all the P_u^{L}; $\boldsymbol{P}^{\mathrm{N}}$ is the vector of all the nodal active power injections denoted by P_n^{N}; and $\boldsymbol{\sigma}$ is a constant coefficient matrix that can be calculated by branch impedances [31] or identified from the measurements of $\boldsymbol{P}^{\mathrm{L}}$ and $\boldsymbol{P}^{\mathrm{N}}$ [32].

3) Line Loading Indicators Under N–1 Contingencies

Assume that $P_{\mathcal{G}-g,u}^{\mathrm{L}}$ denotes the active power flow of line u under the contingency of generator g, whose security threshold is denoted as $P_{u,\max}^{\mathrm{L}}$. $P_{\mathcal{G}-g,u}^{\mathrm{L}}$ can be calculated by power transfer distribution factors (PTDFs) as:

$$P_{\mathcal{G}-g,u}^{\mathrm{L}} = P_u^{\mathrm{L}} + \sum_{p \in \mathcal{G} \setminus \{g\}} \delta_{n_p, n_g, u} \gamma(p, g) x_g \tag{3}$$

where $\gamma(p, g)$ is a given participation factor of generator p under the contingency of generator g; $\mathcal{G} \setminus \{g\}$ is a set contains all the generators excepted for generator g; and $\delta_{n_p, n_g, u}$ is the change of line loading in line u when transferring 1.0 p.u. of active power from generator p at bus n_p to generator g at bus n_g, which can be calculated by $\boldsymbol{\sigma}$:

$$\delta_{n_p, n_g, u} = \sigma_{u, n_p} - \sigma_{u, n_g} \tag{4}$$

where $\sigma_{u,n}$ is the element at row u and column n of $\boldsymbol{\sigma}$.

The active power in line u under the contingency of line l is denoted as $P_{\mathcal{L}-l,u}^{\mathrm{L}}$, whose security threshold is $P_{u,\max}^{\mathrm{L}}$. $P_{\mathcal{L}-l,u}^{\mathrm{L}}$ can be calculated as:

$$P_{\mathcal{L}-l,u}^{\mathrm{L}} = P_u^{\mathrm{L}} + \eta_{u,l} P_l^{\mathrm{L}} \tag{5}$$

where $\eta_{u,l}$ is the line outage distribution factor (LODF), which indicates the change of line loading in line u after an outage of line l and can be calculated by:

$$\eta_{u,l} = \frac{\delta_{n_l, m_l, u}}{1 - \delta_{n_l, m_l, l}} \tag{6}$$

where n_l and m_l are the from-bus and to-bus of line l, respectively.

4) Small-signal Stability Indicators

The small-signal stability refers to the system ability to suppress power system oscillations caused by small perturbations [33]. For a dominant oscillation mode j, the damping ratio ζ_j is defined as a small-signal stability indicator that can be obtained by online oscillation damping monitoring [34]. In general, if one damping ratio is lower than 3%, it means the system is underdamped. In this paper, the corresponding security threshold is set to be 3% to leave a margin.

In practice, damping ratios are often formulated as local linearized functions for a single operation point in real-time dispatch.

B. Ideal Operation Point of Power System

The fundamental goal of power system dispatch is to achieve an ideal operation point through a series of dispatch actions. This destination can be determined according to the following three principles.

1) All security requirements and other constraints should be satisfied.

2) The Pareto optimization of all the indicators presented in Section III-A should be attained.

3) The generation cost should be minimized without violating principles 1) and 2).

Thus, the dispatch problem can be formulated as:

$$\begin{cases} \min f(\boldsymbol{x}) \\ \text{s.t.} \quad \boldsymbol{x} \in \boldsymbol{S} \end{cases} \tag{7}$$

where $\boldsymbol{S}$ is the Pareto solution set of (8).

$$\begin{cases} \min [f, \boldsymbol{P}^{\mathrm{L}}, \boldsymbol{P}_{\mathcal{G}}^{\mathrm{L}}, \boldsymbol{P}_{\mathcal{L}}^{\mathrm{L}}, -\boldsymbol{\zeta}]^{\mathrm{T}} \\ \sum_{g=1}^{G} x_g + \sum_{d=1}^{D} P_d^{\mathrm{D}} + P^{\mathrm{LOSS}} = 0 \\ x_g \le x_{g,\max} \quad \forall g \in \mathcal{G} \\ P_u^{\mathrm{L}}(\boldsymbol{x}) \le P_{u,\max}^{\mathrm{L}} \quad \forall u \in \mathcal{L} \\ P_{\mathcal{G}-g,u}^{\mathrm{L}}(\boldsymbol{x}) \le P_{u,\max}^{\mathrm{L}} \quad \forall g \in \mathcal{G} \\ P_{\mathcal{L}-l,u}^{\mathrm{L}}(\boldsymbol{x}) \le P_{u,\max}^{\mathrm{L}} \quad \forall l \in \mathcal{L} \\ \zeta_j(\boldsymbol{x}) \ge 3\% \quad \forall j \in \mathcal{J} \end{cases} \tag{8}$$

where $\boldsymbol{P}_{\mathcal{G}}^{\mathrm{L}}$ and $\boldsymbol{P}_{\mathcal{L}}^{\mathrm{L}}$ are the vectors of line loading indicators in N–1 conditions; P_d^{D} is the load demand of load d; $\boldsymbol{\zeta}$ is the vector of the damping ratios for all the dominant oscillation modes of the system; $x_{g,\max}$ is the installed capacity of generator g; and P^{LOSS} is the total active power loss in the system, which can be approximated to a linear function of $\boldsymbol{x}$.

The proposed optimization model can be shown schematically in Fig. 4, where the Pareto front of (8) is represented as arc BC, while the optimal solution of (7) is represented as point B. Arc BE is the optimal solution set of a model consisting of the objective function in (7) and the constraints in (8), which is widely used as conventional dispatch models. In some situations, the arc BE can degenerate to a single point, which means that there is only one solution that can optimize the generation cost while satisfying all the security constraints. In this case, the proposed model is equivalent to the conventional model. In other situations, for example, if

there are two dispatchable active sources with the same linear cost function but different sensitivities to some security indicators, or if the generation cost functions of generators are designed to be piecewise or fuzzy to ignore small cost differences, there may be two or more operation points with the same generation cost but different security margins. All of these operation points satisfy all the security constraints. In this case, the proposed model can choose the safer one from them.

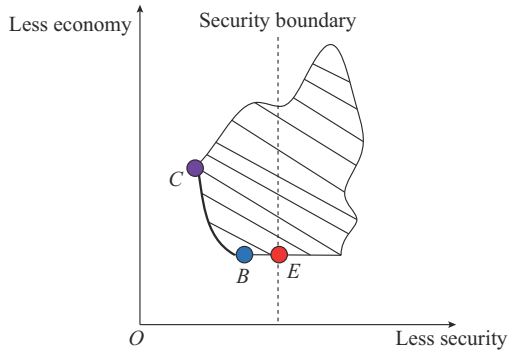

Fig. 4. Feasible region and Pareto front of the proposed model.

C. Ideal Dispatch Decision for Each Decision Moment

Conventional measurement-based real time dispatch solutions normally try to solve (7) continuously in real time to ensure that the system operation point can meet the principles given in Section III-B, such as the approach presented in [7]. However, because the conventional thermal generators have ramp limitations in practice, the solution of (7) may not be able to reach within one period of the real-time dispatch. In this case, if the ramp limitations as constraints are directly added to (7), the problem would easily become unsolvable and lead to constraint violation problems. Therefore, this study does not try to solve (7) directly in each step of optimization, but only ensure that the system can approach the solution of (7) in a suitable path.

The following characteristics should be considered to plan for a path to reduce the duration of the constraint violations.

1) The chosen path should connect the current operation point and the solution of (7).

2) The portion outside the security boundary should be as short as possible.

As the uncertain fluctuations of load demands and other operation conditions on a very short time scale are unpredictable, it is difficult to plan for an optimal path with the presented characteristics in advance like what the prediction-based dispatch on a longer time scale does. Instead, the dispatch decision is optimized at each step to form an acceptable path meeting the above requirements. Thus, the dispatch decision for a single dispatch period should be made according to the following three principles.

1) The gaps between the unsatisfied security requirements and their security thresholds should be as narrow as possible.

2) The generation cost should be minimized without violating principle 1).

3) The satisfied security requirements should be improved as much as possible without violating principles 1) and 2).

Thus, the presented dispatch problem for every single decision moment of real-time dispatch can be formulated as:

$$\begin{cases}\min f(\boldsymbol{x}) \\ \text{s.t. } \boldsymbol{x}\in\boldsymbol{S}'\end{cases} \tag{9}$$

where $\boldsymbol{S}'$ is a subset of the Pareto solution set of (10).

$$\begin{cases}\min[f,\boldsymbol{P}^{\mathrm{L}},\boldsymbol{P}^{\mathrm{L}}_{\mathcal{G}},\boldsymbol{P}^{\mathrm{L}}_{\mathcal{L}},-\boldsymbol{\zeta}]^{\mathrm{T}} \\ \text{s.t. } \boldsymbol{x}\in\boldsymbol{S}''\end{cases} \tag{10}$$

where $\boldsymbol{S}''$ is a subset of the Pareto solution set of (11).

$$\begin{cases}\min[\boldsymbol{P}^{\mathrm{L,gap}},\boldsymbol{P}^{\mathrm{L,gap}}_{\mathcal{G}},\boldsymbol{P}^{\mathrm{L,gap}}_{\mathcal{L}},-\boldsymbol{\zeta}^{\mathrm{gap}}]^{\mathrm{T}} \\ \text{s.t. } \boldsymbol{P}^{\mathrm{L,gap}},\boldsymbol{P}^{\mathrm{L,gap}}_{\mathcal{G}},\boldsymbol{P}^{\mathrm{L,gap}}_{\mathcal{L}},\boldsymbol{\zeta}^{\mathrm{gap}}\ge\boldsymbol{0} \\ \quad \sum_{g=1}^{G}x_g+\sum_{d=1}^{D}P_d^{\mathrm{D}}+P^{\mathrm{LOSS}}=0 \\ \quad \left|x_g-x_{g,0}\right|\le x_{g,\mathrm{ramp}} \quad \forall g\in\mathcal{G} \\ \quad P_u^{\mathrm{L}}(\boldsymbol{x})\le P_{u,\max}^{\mathrm{L}}+P_u^{\mathrm{L,gap}} \quad \forall u\in\mathcal{L} \\ \quad P_{\mathcal{G}-g,u}^{\mathrm{L}}(\boldsymbol{x})\le P_{u,\max}^{\mathrm{L}}+P_{\mathcal{G}-g,u}^{\mathrm{L,gap}} \quad \forall g\in\mathcal{G} \\ \quad P_{\mathcal{L}-l,u}^{\mathrm{L}}(\boldsymbol{x})\le P_{u,\max}^{\mathrm{L}}+P_{\mathcal{L}-l,u}^{\mathrm{L,gap}} \quad \forall l\in\mathcal{L} \\ \quad \zeta_j(\boldsymbol{x})+\zeta_j^{\mathrm{gap}}\ge 3\% \quad \forall j\in\mathcal{J}\end{cases} \tag{11}$$

where $P_u^{\mathrm{L,gap}}\in\boldsymbol{P}^{\mathrm{L,gap}}$, $P_{\mathcal{G}-g,u}^{\mathrm{L,gap}}\in\boldsymbol{P}_{\mathcal{G}}^{\mathrm{L,gap}}$, $P_{\mathcal{L}-l,u}^{\mathrm{L,gap}}\in\boldsymbol{P}_{\mathcal{L}}^{\mathrm{L,gap}}$, and $\zeta_j^{\mathrm{gap}}\in\boldsymbol{\zeta}^{\mathrm{gap}}$ are the gaps between the unsatisfied security requirements and their security thresholds; $x_{g,\mathrm{ramp}}$ is the ramp limitation of generator g within the time scale of a single real-time dispatch; and $x_{g,0}$ is the initial value of x_g at the beginning of this step of real-time dispatch.

Unlike model (7), model (9) gives priority to narrowing down security thresholds. Only if there is more than one operation point which can narrow down security thresholds as much as possible, the proposed model will then consider the economic indicator.

In practice, the constraint violations with larger threats need to be prioritized. In that case, instead of the whole Pareto solution set, $\boldsymbol{S}'$ and $\boldsymbol{S}''$ will use a subset of the Pareto solution set that considers the priority of security indicators.

Because $x_{g,\mathrm{ramp}}$ is very small for the very short time scale of real-time dispatch, $\boldsymbol{\zeta}(\boldsymbol{x})$ can be approximated by a locally linearized model as:

$$\boldsymbol{\zeta}(\boldsymbol{x})=\boldsymbol{\zeta}_0+\boldsymbol{S}_{\zeta\mathrm{G}}(\boldsymbol{x}-\boldsymbol{x}_0) \tag{12}$$

where $\boldsymbol{\zeta}_0$ is the damping ratio vector of the current operation point; $\boldsymbol{x}_0$ is the initial value vector of $\boldsymbol{x}$ at the beginning of current step of real-time dispatch; and $\boldsymbol{S}_{\zeta\mathrm{G}}$ is the sensitivity matrix of damping ratios with respect to the active power generation. $\boldsymbol{S}_{\zeta\mathrm{G}}$ can be calculated directly if a detailed dynamic model of the system can be obtained; otherwise, it can be identified with the real-time measurement by using eigenvalue sensitivity methods, which are well studied in [8]. Now all of the security indicators in the model are formulated by a linear function.

IV. Solution Methods

The dynamic-decision-based real-time dispatch model presented in Section III is a multi-objective optimization problem with a complex hierarchical structure, where the choice of the subsets $\boldsymbol{S}'$ and $\boldsymbol{S}''$ determines the dispatch decision.

This section presents a multi-step method to determine the subsets and solve the model in real time.

The implementation of the seven key steps is as follows. λ_1, λ_2, and λ_3 are the queues created for storing the security indicators. λ_1 stores the indicators to be optimized, λ_2 stores the indicators that have already been optimized in the current dispatch, and λ_3 stores the indicators that have already satisfied their constraints. Denote λ_1^0, λ_2^0, and λ_3^0 as the first elements of the queues. For a single indicator I, denote its initial value as $I_{V_1}=I(\boldsymbol{x}_0)$, its optimized value as I_{V_2}, and its corresponding security threshold as I_{V_3}.

Step 1: identify model parameters.

The parameters matrices $\boldsymbol{\sigma}$ and $\boldsymbol{S}_{\zeta,\mathrm{G}}$ can be calculated with a detailed model of the system or estimated by historical phasor measurement unit (PMU) data. To avoid the influence of the model error, the latter method is chosen to identify the parameters.

As this paper does not focus on the technical details of the sensitivity estimation, more details are in [7], [8], and [35].

Step 2: calculate security indicators.

The current values of $\boldsymbol{P}^{\mathrm{L}}$ can be measured directly, while $\boldsymbol{P}_{\mathcal{G}}^{\mathrm{L}}$, $\boldsymbol{P}_{\mathcal{L}}^{\mathrm{L}}$, and $\boldsymbol{\zeta}$ can be calculated by (3), (5), and (12) after obtaining $\boldsymbol{\sigma}$ and $\boldsymbol{S}_{\zeta,\mathrm{G}}$ in *Step 1*. By comparing the current values and thresholds of the security indicators, the unsatisfied security requirements and the enqueue of the corresponding indicators can be screened out into λ_1 to be optimized, while other indicators are enqueued to λ_3.

Step 3: order the indicators in λ_1 in reverse order of priority.

The priority of security indicators should be evaluated considering the type of security requirements, the severity of the over-limits, and the expert knowledge in practice. In this paper, the following evaluation criteria are used.

1) Priority order among different categories of indicators (high to low) is line loading, damping ratio (smaller than 3%), line loading in the N–1 condition, and damping ratio (smaller than 5%).

2) Priority order of the same category of indicators depends on the priority indicator $I_{\mathrm{priority1}}$ calculated by (13).

$$I_{\mathrm{priority1}}=\frac{I_{V_3}-I_{V_1}}{I_{V_3}}\times 100\% \tag{13}$$

Step 4: optimize λ_1^0.

Dequeue λ_1^0, which is the indicator with the highest priority in λ_1, and optimize it by (14).

$$\begin{cases}\min\ \lambda_1^0(\boldsymbol{x})\\ \text{s.t.}\ \ \sum_{g=1}^{G}x_g+\sum_{d=1}^{D}P_d^{\mathrm{D}}+P^{\mathrm{LOSS}}=0\\ \quad \left|x_g-x_{g,0}\right|\le x_{g,\mathrm{ramp}}\quad \forall g\in\mathcal{G}\\ \quad I^{\mathrm{I}}(\boldsymbol{x})\le I_{V_1}^{\mathrm{I}}\quad \forall I^{\mathrm{I}}\in\lambda_1\\ \quad I^{\mathrm{II}}(\boldsymbol{x})\le I_{V_2}^{\mathrm{II}}\quad \forall I^{\mathrm{II}}\in\lambda_2\\ \quad I^{\mathrm{III}}(\boldsymbol{x})\le I_{V_3}^{\mathrm{III}}\quad \forall I^{\mathrm{III}}\in\lambda_3\end{cases} \tag{14}$$

where I^{I}, I^{II}, and I^{III} are the indicators contained in λ_1, λ_2, and λ_3, respectively. For a single indicator I^j, denote its initial value as $I_{V_1}^j=I^j(\boldsymbol{x}_0)$, its optimized value as $I_{V_2}^j$, and its corresponding security threshold as $I_{V_3}^j$.

For a single indicator λ_j^k, denote its initial value as $\lambda_{j,V_1}^k=\lambda_j(\boldsymbol{x}_0)$, its optimized value as λ_{j,V_2}^k, and its corresponding security threshold as λ_{j,V_3}^k. Set the λ_{1,V_2}^0 to be the optimal value obtained by (14), then move λ_1^0 to λ_2 if $\lambda_{1,V_2}^0<\lambda_{1,V_3}^0$; otherwise, move λ_1^0 to λ_3. Repeat this process until λ_1 is empty.

Step 5: optimize the generation cost.

After all of the indicators in λ_1 have been moved to λ_2 or λ_3, none of the gaps towards unsatisfied security requirements can be further optimized without sacrificing others. By fixing all of the bound values in (14), a subset of the Pareto solution set of (11) considering the priority order given in key *Step 3* is determined, which can be used as $\boldsymbol{S}''$ in (10). On this basis, the generation cost should be optimized by (15).

$$\begin{cases}\min f(\boldsymbol{x})\\ \text{s.t.}\ \ \sum_{g=1}^{G}x_g+\sum_{d=1}^{D}P_d^{\mathrm{D}}+P^{\mathrm{LOSS}}=0\\ \quad \left|x_g-x_{g,0}\right|\le x_{g,\mathrm{ramp}}\quad \forall g\in\mathcal{G}\\ \quad I^{\mathrm{II}}(\boldsymbol{x})\le I_{V_2}^{\mathrm{II}}\quad \forall I^{\mathrm{II}}\in\lambda_2\\ \quad I^{\mathrm{III}}(\boldsymbol{x})\le I_{V_3}^{\mathrm{III}}\quad \forall I^{\mathrm{III}}\in\lambda_3\end{cases} \tag{15}$$

Denote the optimal solution of (15) as $\boldsymbol{x}'$, which will be used in subsequent steps. Though the optimal solution solved in (15) is a Pareto solution of (11), it may not be a Pareto solution of (10) for some of the security indicators that can be further optimized after its security constraint is met. These indicators will be handled in the following steps.

Step 6: order the indicators in λ_3 in reverse order of priority.

The evaluation of priority among indicators in λ_3 is similar to those in λ_1.

1) Priority order among different categories of indicators (high to low) is that line loading in the N–1 condition is superior to damping ratio. The order of line loading indicators and N–1 indicators changes because N–1 indicators are often more critical than line loading indicators.

2) Priority order of the same category of indicators depends on the priority indicator $I_{\mathrm{priority2}}$ calculated by (16).

$$I_{\mathrm{priority2}}=\frac{I_{V_3}-I(\boldsymbol{x}')}{I_{V_3}}\times 100\% \tag{16}$$

Step 7: optimize λ_3^0.

Dequeue λ_3^0, and then optimize it by (17). Set λ_{3,V_2}^0 to be the optimal value obtained from (17), then move λ_3^0 to λ_2. Repeat this process until λ_3 is empty, then set the optimal solution $\boldsymbol{x}''$ of (17) in the last loop as the active reference.

$$\begin{cases} \min \lambda_3^0(\boldsymbol{x}) \\ \text{s.t.} \quad \sum_{g=1}^{G} x_g + \sum_{d=1}^{D} P_d^{\mathrm{D}} + P^{\mathrm{LOSS}} = 0 \\ \quad f(\boldsymbol{x}) \le f(\boldsymbol{x}') \\ \quad \left| x_g - x_{g,0} \right| \le x_{g,\mathrm{ramp}} \quad \forall g \in \mathcal{G} \\ \quad I^{\mathrm{II}}(\boldsymbol{x}) \le I_{V_2}^{\mathrm{II}} \quad \forall I^{\mathrm{II}} \in \lambda_2 \\ \quad I^{\mathrm{III}}(\boldsymbol{x}) \le I_{V_3}^{\mathrm{III}} \quad \forall I^{\mathrm{III}} \in \lambda_3 \end{cases} \tag{17}$$

After all the indicators have been moved to λ_2, none can be further optimized without sacrificing others. In that case, $\boldsymbol{x}''$ is a Pareto solution of (10) with the minimum generation cost, so it is also the optimal solution of (9).

Because both (15) and (17) are linear programming problems that can be solved in polynomial time, the presented solution can be efficiently calculated on a time scale that meets the requirement for the real-time implementation.

V. Case Studies

The IEEE 39-bus system [36] is used to evaluate the effectiveness of the proposed method for the real-time dispatch problem. The parameters of the power system stabilizers (PSSs) in the system have not been well tuned to ensure the small-signal stability.

Because the system has 10 generators and 34 branches, there will be 340 (34×10) line loading indicators under single-generator contingencies as well as 1156 (34×34) line loading indicators under single-line contingencies. With the additional small-signal stability indicators of eight dominant oscillation modes with small damping ratios, a total of 1504 security indicators need to be considered.

The time resolution of the intra-hour dispatch module is assumed to be 15 min, which means that the effect of uncertain load fluctuations within 15 min should be dampened by the dispatch modules with a shorter time scale. In this paper, this task is undertaken by the real-time dispatch approach. The time resolution of real-time dispatch is set to be 1 min. The parameters a_g and b_g in the generation cost function (1) are defined as $a_g \in \boldsymbol{a}$ =[0.11, 0.10, 0.09, 0.12, 0.10, 0.11, 0.13, 0.11, 0.10, 0.10]$^{\mathrm{T}}$ and $b_g \in \boldsymbol{b}$ = [3.4040, 4.56, 1.43, 2.30, 1.60, 2.29, 2.88, 3.35, 2.67]$^{\mathrm{T}}$, respectively.

PowerFactory-DIGSILENT is used as the simulation platform. The simulation step size is set to be 30 steps per second, which is the same as the sampling period of a PMU. A small uniform distribution random perturbation is added to all of the loads in every step to simulate the micro-disturbance of loads [7]. In every simulation step, a set of power flow results and damping ratios is calculated and contaminated with noise to simulate measured or identified data. The active power injections of buses, generators, and loads, as well as branch active power flows and damping ratios, will be recorded every step, where the damping ratios are assumed to be obtained from the online oscillation damping monitoring systems [33], [34]. The model parameters will be identified with these data at the beginning of dispatch using the methods presented in [7], [8], and [35].

Three cases are provided to verify the performance of the solution proposed in this paper. Case 1 verifies if the proposed method can consider all types of security indicators; case 2 verifies if the proposed method can reduce the constraints violations while driving the system to the optimal opertion point with a static operation condition; and case 3 provides a large sample experiment with continuously varying random operation conditions to check if the proposed method can reduce the constraint violations.

A. Case 1

The real-time security-constrained ED (SCED) presented in [7] and the real-time small-signal stability constrained ED (SSSC-ED) presented in [8] are chosen as benchmarks. In addition to the sensitivity-based methods mentioned above, a test case without any real-time dispatch is also performed, in which all generators compensate for the load fluctuations and the proportion of gross generation for each generator stays the same. As described in Section II, only the measurement-based single dispatch strategies can adjust the deviation caused by both model errors and unpredictable power flow fluctuations. In this case, only the dispatch strategies reported in [7] and [8] have comparability with the proposed method among all the reported dispatch strategies.

The net loads at the transmission level are modeled as fluctuating time series, as shown in Fig. 5. Since this paper focuses on the dispatch methods instead of the modeling of distribution networks, an aggregated *P*-*Q* model is used to represent the complex dynamic distribution system.

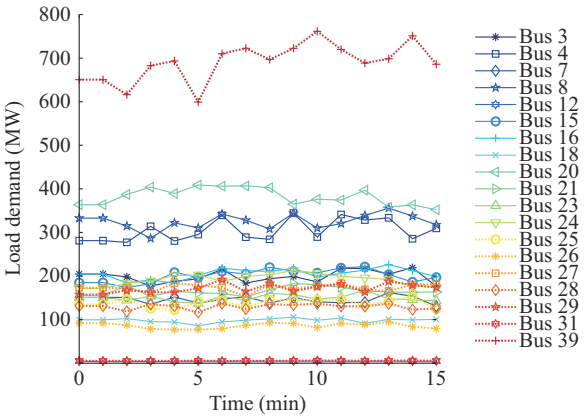

Fig. 5. Load fluctuation of each load within 15 min.

B. Case 2

This case provides a more intuitive example to show the trajectory of the operation point under different real-time dispatch solutions. The initial operation point is shown in Fig. 6.

In this case, the line loading of branch 6-11 under the contingency of branch 13-14 will be out of limit, which cannot be maintained in a single step of real-time dispatch under the ramp limitation of 2% per minute. The proposed method and the SCED method are used as respective real-time dispatch solutions to maintain the *N*–1 indicator and minimize the power loss. Since SCED does not consider the ramp limitation, the unattainable change in power generation will be slacked by other generators.

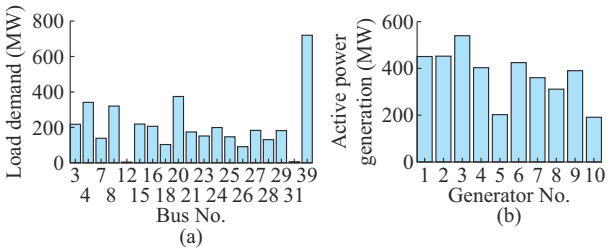

Fig. 6. Initial operation point of case II. (a) Load demand. (b) Active power generation.

C. Case 3

Case 1 is proposed to verify whether the proposed method can handle the multiple types of dispatch indicators, while case 2 verifies whether the system can finally reach the optimal operation point through a safer path by the proposed dynamic decision than by the existing dispatch strategy. Case 3 wants to verify the proposed method in a broader way. One hundred random processes are generated, where each process lasts 15 min and the initial condition is the same as that of case 1. For each process, the power flow will change every 1 min by adding a random value of –10% to 10% of its previous value under the uniform distribution. The step size of the power dispatch is also 1 min. The proposed method is compared with the measurement-based method without a dynamic decision.

D. Discussion on Case Results

As shown in Figs. 7 and 8, the *N*–1 indicators and the small-signal stability objectives are both frequently out of limit without the real-time dispatch in case 1. The real-time SCED can maintain *N*–1 security but leads to a more serious small-signal stability problem. The real-time SSSC-ED can maintain the small-signal stability within two dispatch steps but seriously worsens the *N*–1 constraints. Only the proposed method can address both the *N*–1 and small-signal stability problems. As shown in Fig. 9, the total generation cost of the proposed method is much lower than that of the one without dispatch and similar to that of SSSC-ED. The SCED has better performance in terms of cost reduction, but the price is severe underdamping.

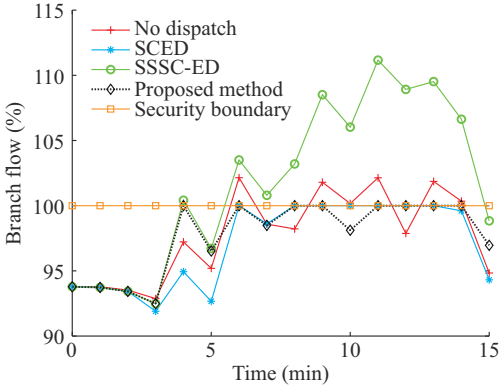

Fig. 7. The highest branch flow loading under *N*–1 conditions in case 1.

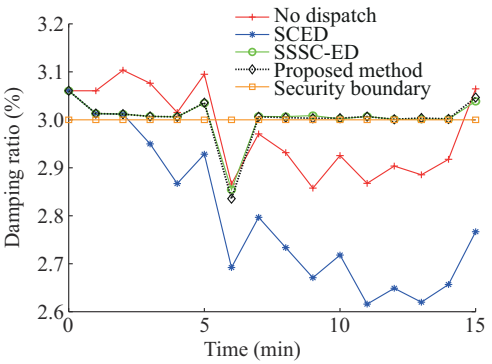

Fig. 8. The minimum damping ratio in case 1.

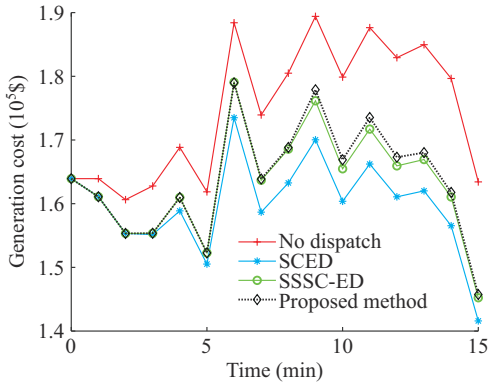

Fig. 9. Total generation costs in case 1.

Case 1 shows the proposed method can simultaneously consider multiple kinds of objectives and perform dispatch methods that can only focus on one type of objective, with a small rise in generation cost.

The simulation results of case 2 are shown in Figs. 10 and 11. Both the proposed method and SCED reach the operation point with total generation costs minimized and the *N*–1 security requirement satisfied, but the proposed method can reach the security region within five intervals while the SCED method needs eight steps. The results show that the proposed method can move the operation point by a more secure way to the optimum.

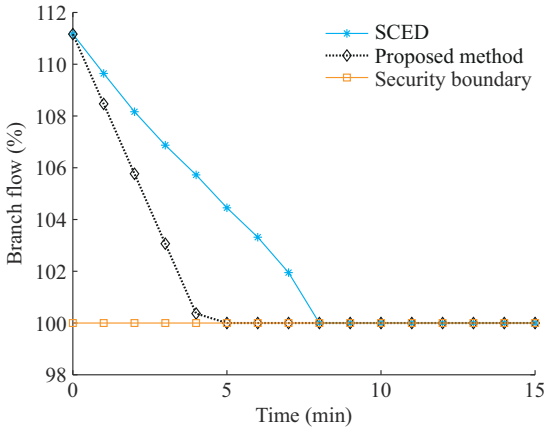

Fig. 10. The highest branch flow loading under *N*–1 conditions in case 2.

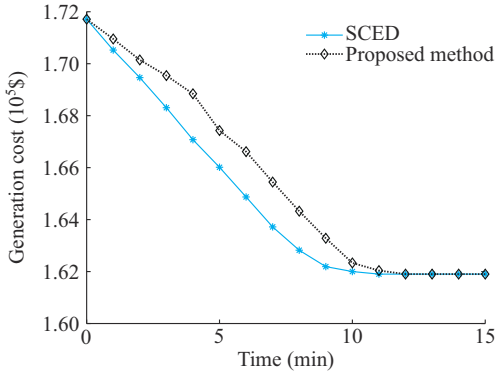

Fig. 11. Total generation costs in case 2.

For case 3, the constraint violations of the worst N–1 line loadings and the smallest damping ratios in the 100 samples are shown in Figs. 12 and 13, which indicate that the proposed method can effectively reduce the severity of constraint violations under different situations.

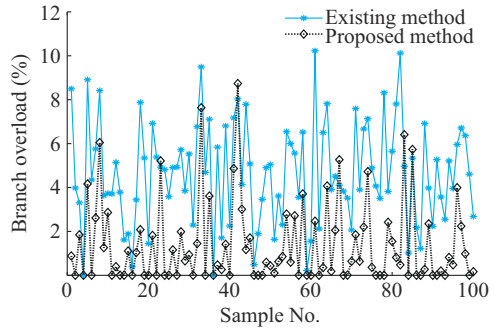

Fig. 12. Constraint violations of the worst N–1 line loadings in 100 samples.

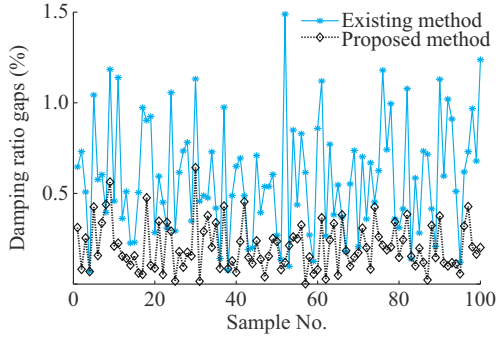

Fig. 13. Constraint violations of the smallest damping ratios in 100 samples.

For case 3, a constraint violation indicator (CVI) is proposed with the formulation of (18) to evaluate the severity of constraint violations.

$$\theta(s)=\sum_{t=1}^{t_{\max}}(s(t)-s_{\text{th}})_{+} \tag{18}$$

where s is a type of security objective; s_{th} is the security threshold of s; $s(t)$ is the actual value of the security objective at time t; $t_{\max}$ is the total simulation time; $(\cdot)_{+}$ is an operator to change all the negative values to zero; and θ is the time integral of security objective violations. The CVI of the worst N–1 line loadings and the smallest damping ratios in the 100 samples are shown in Figs. 13 and 14, which shows that the proposed method can effectively reduce the constraint violations under different situations.

Regarding the computation performance, a 2.20 GHz CPU is used to estimate the sensitivity matrices and solve all the optimal problems. The time cost of all the calculations is less than 0.5 s for any calculation period, which is fast enough to allow the method to work in real time. For larger systems, since (15) and (17) are both linear programming, developed algorithms for solving linear programming problems can be used to ensure the real-time performance.

VI. Conclusion

This paper establishes a new dynamic-decision-based real-time dispatch method to reduce constraint violations during the dispatch process before the system reaches the optimal operation point. The proposed method considers the priorities of different dispatch objectives including generation cost, N–1 line loading, and damping ratios of the system at different operation points. At each decision moment, the proposed method first narrows down the gaps between the unsatisfied security requirements and their security thresholds as much as possible, then minimizes the generation cost without widening the gaps or causing new unsatisfied constraints. Finally, the margin for the satisfied security requirements is optimized. The proposed method is evaluated with the IEEE 39-bus system and the results demonstrate that the proposed method can move the operation point of the system to an optimal solution considering multiple security indicators as well as significantly reduce constraint violations. In particular, the proposed method only takes 62.5% of the time to eliminate constraint violations of the N–1 line loading compared with the SCED method. A randomized controlled simulation with 100 samples shows the superiority of the proposed method under different situations with drastic power fluctuations.

References

[1] Q. Wang, A. Yang, F. Wen *et al.*, "Risk-based security-constrained economic dispatch in power systems," *Journal of Modern Power Systems and Clean Energy*, vol. 1, no. 2, pp. 142-149, Sept. 2013.
[2] E. Marris, "Energy: upgrading the grid," *Nature*, vol. 454, no. 7204, pp. 570-573, Jul. 2008.
[3] D. N. Kosterev, C. W. Taylor, and W. A. Mittelstadt, "Model validation for the August 10 1996 WSCC system outage," *IEEE Transactions on Power Systems*, vol. 14, no. 3, pp. 967-979, Aug. 1999.
[4] L. Che, X. Liu, X. Zhu *et al.*, "Intra-interval security based dispatch for power systems with high wind penetration," *IEEE Transactions on Power Systems*, vol. 34, no. 2, pp. 1243-1255, Mar. 2019.
[5] B. Khorramdel, A. Zare, C. Y. Chung *et al.*, "A generic convex model for a chance-constrained look-ahead economic dispatch problem incorporating an efficient wind power distribution modeling," *IEEE Transactions on Power Systems*, vol. 35, no. 2, pp. 873-886, Mar. 2020.
[6] X. Zheng, H. Chen, Y. Xu *et al.*, "A hierarchical method for robust SCUC of multi-area power systems with novel uncertainty sets," *IEEE Transactions on Power Systems*, vol. 35, no. 2, pp. 1364-1375, Mar. 2020.
[7] K. E. van Horn, A. D. Domínguez-García, and P. W. Sauer, "Measurement-based real-time security-constrained economic dispatch," *IEEE Transactions on Power Systems*, vol. 31, no. 5, pp. 3548-3560, Sept. 2016.
[8] J. Zhang, C. Lu, C. Y. Chung *et al.*, "Online re-dispatching of power

systems based on modal sensitivity identification," *IET Generation Transmission & Distribution*, vol. 9, no. 12, pp. 1352-1360, Sept. 2015.
[9] G. Wang, Z. Li, F. Zhang *et al*., "Data-driven probabilistic static security assessment for power system operation using high-order moments," *Journal of Modern Power Systems and Clean Energy*, vol. 9, no. 5, pp. 1233-1236, Sept. 2021.
[10] P. Li, Y. Wei, J. Qi *et al*., "A closed-form formulation of eigenvalue sensitivity based on matrix calculus for small-signal stability analysis in power system," *Journal of Modern Power Systems and Clean Energy*, vol. 9, no. 6, pp. 1436-1445, Nov. 2021.
[11] P. Carpentier, G. Gohen, J. Culioli *et al*., "Stochastic optimization of unit commitment: a new decomposition framework," *IEEE Transactions on Power Systems*, vol. 11, no. 2, pp. 1067-1073, May 1996.
[12] J. Hetzer, D. Yu, and K. Bhattarai, "An economic dispatch model incorporating wind power," *IEEE Transactions on Energy Conversion*, vol. 23, no. 2, pp. 603-611, Jun. 2008.
[13] L. Yang, M. He, V. Vittal *et al*., "Stochastic optimization-based economic dispatch and interruptible load management with increased wind penetration," *IEEE Transactions on Smart Grid*, vol. 7, no. 2, pp. 730-739, Mar. 2016.
[14] Z. Li, W. Wu, B. Zhang *et al*., "Adjustable robust real-time power dispatch with large-scale wind power integration," *IEEE Transactions on Sustainable Energy*, vol. 6, no. 2, pp. 357-368, Apr. 2015.
[15] P. Srikantha and D. Kundur, "A game theoretic approach to real-time robust distributed generation dispatch," *IEEE Transactions on Industrial Informatics*, vol. 13, no. 3, pp. 1006-1016, Jun. 2017.
[16] A. Zhou, M. Yang, Z. Wang *et al*., "A linear solution method of generalized robust chance constrained real-time dispatch," *IEEE Transactions on Power Systems*, vol. 33, no. 6, pp. 7313-7316, Nov. 2018.
[17] W. Zhang, W. Liu, X. Wang *et al*., "Online optimal generation control based on constrained distributed gradient algorithm," *IEEE Transactions on Power Systems*, vol. 30, no. 1, pp. 35-45, Jan. 2015.
[18] R. Patel, C. Li, L. Meegahapola *et al.*, "Enhancing optimal automatic generation control in a multi-area power system with diverse energy resources," *IEEE Transactions on Power Systems*, vol. 34, no. 5, pp. 3465-3475, Sept. 2019.
[19] Y. Jia, Z. Y. Dong, C. Sun *et al.*, "Cooperation-based distributed economic MPC for economic load dispatch and load frequency control of interconnected power systems," *IEEE Transactions on Power Systems*, vol. 34, no. 5, pp. 3964-3966, Sept. 2019.
[20] O. Alsaç and B. Stott, "Optimal load flow with steady-state security," *IEEE Transactions on Power Apparatus Systems*, vol. 93, no. 3, pp. 745-751, May 1974.
[21] A. Gupta and C. L. Anderson, "Statistical bus ranking for flexible robust unit commitment," *IEEE Transactions on Power Systems*, vol. 34, no. 1, pp. 236-245, Jan. 2019.
[22] C. He, L. Wu, T. Liu *et al*., "Robust co-optimization planning of interdependent electricity and natural gas systems with a joint *N*–1 and probabilistic reliability criterion," *IEEE Transactions on Power Systems*, vol. 33, no. 2, pp. 2140-2154, Mar. 2018.
[23] A. Zhou, M. Yang, M. Wang *et al*., "A linear programming approximation of distributionally robust chance-constrained dispatch with Wasserstein distance," *IEEE Transactions on Power Systems*, vol. 35, no. 5, pp. 3366-3377, Sept. 2020.
[24] M. S. Modarresi, L. Xie, M. C. Campi *et al*., "Scenario-based economic dispatch with tunable risk levels in high-renewable power systems," *IEEE Transactions on Power Systems*, vol. 34, no. 6, pp. 5103-5114, Nov. 2019.
[25] P. Li, M. Yang, and Q. Wu, "Confidence interval based distributionally robust real-time economic dispatch approach considering wind power accommodation risk," *IEEE Transactions on Sustainable Energy*, vol. 12, no. 1, pp. 58-61, Jan. 2021.
[26] J. Condren and T. W. Gedra, "Expected-security cost optimal power flow with small-signal stability constraints," *IEEE Transactions on Power Systems*, vol. 21, no. 4, pp. 1736-1743, Nov. 2006.
[27] R. Zárate-Miñano, F. Milano, and A. J. Conejo, "An OPF methodology to ensure small-signal stability," *IEEE Transactions on Power Systems*, vol. 26, no. 3, pp. 1050-1061, Aug. 2011.
[28] P. Li, J. Qi, J. Wang *et al*., "An SQP method combined with gradient sampling for small-signal stability constrained OPF," *IEEE Transactions on Power Systems*, vol. 32, no. 3, pp. 2372-2381, May 2017.
[29] Y. Li, G. Geng, Q. Jiang *et al*., "A sequential approach for small signal stability enhancement with optimizing generation cost," *IEEE Transactions on Power Systems*, vol. 34, no. 6, pp. 4828-4836, Nov. 2019.
[30] S. Mendoza-Armenta and I. Dobson, "Applying a formula for generator redispatch to damp interarea oscillations using synchrophasors," *IEEE Transactions on Power Systems*, vol. 31, no. 4, pp. 3119-3128, Jul. 2016.
[31] B. Wood, B. Wollenberg, and G. Sheblé, *Power Generation, Operation, and Control*, 3rd ed. New Jersey: John Wiley and Sons, Inc., 2014.
[32] Y. Chen, A. Domínguez-García, and P. Sauer, "Measurement-based estimation of linear sensitivity distribution factors and applications" *IEEE Transactions on Power Systems*, vol. 29, no. 3, pp. 1372-1382, May 2014.
[33] P. Kundur, *Power System Stability and Control*. New York: McGraw-Hill, 1994.
[34] S. A. N. Sarmadi and V. Venkatasubramanian, "Electromechanical mode estimation using recursive adaptive stochastic subspace identification," *IEEE Transactions on Power Systems*, vol. 29, no. 1, pp. 349-358, Jan. 2014.
[35] J. Zhang, Z. Wang, X. Zheng *et al.*, "Locally weighted ridge regression for power system online sensitivity identification considering data collinearity," *IEEE Transactions on Power Systems*, vol. 33, no. 2, pp. 1624-1633, Mar. 2018.
[36] T. Athay, R. Podmore, and S. Virmani, "A practical method for the direct analysis of transient stability," *IEEE Transactions on Power Apparatus Systems*, vol. 98, no. 2, pp. 573-584, Mar. 1979.

Lingshu Zhong received the B.Eng. and M.Sc. degrees from the South China University of Technology, Guangzhou, China, in 2013 and 2016, respectively. He received the Ph.D. degree at the same university. He was also a visiting Ph.D. student of the University of Saskatchewan, Saskatoon, Canada, from 2018 to 2019. His research interests include power system analysis, operation, and control.

Junbo Zhang received the B.S. and Ph. D. degrees in Electrical Engineering from Tsinghua University, Beijing, China, in 2008 and 2013, respectively. He visited the Hong Kong Polytechnic University, Hong Kong, China and Stanford University, California, USA, from 2009 to 2010 and from 2018 to 2019, respectively. He is currently a Professor at the School of Electric Power, South China University of Technology. His research interests include artificial intelligent in operation and decision making of complex system, knowledge-based expert systems with distributed cloud computing, large-scale industrial software for internet of things, power system simulation with high-performance parallel computing, and power system operation and control.

C. Y. Chung received the B.Eng. (with the First Class Honors) and Ph.D. degrees in electrical engineering from Hong Kong Polytechnic University, Hong Kong, China, in 1995 and 1999, respectively. He is currently a Professor, the NSERC/SaskPower (senior) Industrial Research Chair in smart grid technologies, and the SaskPower Chair in power systems engineering in the Department of Electrical and Computer Engineering at the University of Saskatchewan, Saskatoon, Canada. He is a Senior Editor of IEEE Transactions on Power Systems, Vice Editor-in-chief of Journal of Modern Power Systems and Clean Energy, Subject Editor of IET Generation, Transmission & Distribution, Editor of IEEE Transactions on Sustainable Energy and IEEE Power Engineering Letters, and Editorial Board Member of CSEE Journal of Power and Energy Systems and Protection and Control of Modern Power Systems. He is also an IEEE PES distinguished Lecturer and a member of IEEE PES Fellows Evaluation Committee. His research interests include smart grid technologies, renewable energy, power system stability/control, planning and operation, computational intelligence applications, power markets, and electric vehicle charging.

Yuzhong Gong received the B.S. and Ph.D. degrees in electrical engineering from Zhejiang University of Technology, Hangzhou, China and Zhejiang University, Hangzhou, China, in 2010 and 2015, respectively. He is currently a Post-doctoral Fellow in the Department of Electrical and Computer Engineering, University of Saskatchewan, Saskatoon, Canada. His current research interests include optimization of power system operation, renewable energy integration, and energy storage technologies.

Lin Guan received the B.Eng. and Ph.D. degrees in electrical engineering from Huazhong University of Science and Technology, Wuhan, China, in 1990 and 1995, respectively. She is currently a Professor at the School of Electric Power, South China University of Technology, Guangzhou, China. Her research interests include stability and control of power systems, planning and operation of power systems, and smart grid technologies.